Floquet Mediated Spin Interaction in Weyl Semimetals

Dissertation submitted to

Visvesvaraya National Institute of Technology, Nagpur

in partial fulfillment of the requirements for the award of the degree

Master of Science in Physics

by

Anup Das

under the guidance of

Dr. Sayandip Ghosh

Department of Physics

Visvesvaraya National Institute of Technology, Nagpur

Nagpur 440 010, India

May 2025

Floquet Mediated Spin Interaction in Weyl Semimetals

Dissertation submitted to

Visvesvaraya National Institute of Technology, Nagpur

in partial fulfillment of the requirements for the award of the degree

Master of Science in Physics

by

Anup Das

under the guidance of

Dr. Sayandip Ghosh

Department of Physics

Visvesvaraya National Institute of Technology, Nagpur

Nagpur 440 010, India

May 2025

© Visvesvaraya National Institute of Technology (VNIT), 2025

Department of Physics

Visvesvaraya National Institute of Technology, Nagpur

Dissertation Approval Sheet

Dissertation entitled "Floquet Mediated Spin Interaction in Irradiated Weyl Semimetals" by Anup Das Enrollment No. **MS23PHY016** ID No. 30626 is approved for the degree of Master of Science in Physics

Name:
Supervisor

Name:
External Examiner

Name:
Chairman

Department of Physics
Visvesvaraya National Institute of Technology, Nagpur

Declaration

I, **Anup Das**, hereby declare that this dissertation titled **"Floquet Mediated Spin Interaction in Weyl Semimetals"** is carried out by me in the Department of Physics of Visvesvaraya National Institute of Technology, Nagpur. The work is original and has not been submitted earlier whole or in part for the award of any degree/diploma at this or any other Institution / University.

Anup Das
Date:

Certificate

This is to certify that the dissertation titled **"Floquet Mediated Spin Interaction in Weyl Semimetals"** is submitted by **Anup Das** in partial fulfillment of the requirements for the award of the degree of **Master of Science in Physics**, VNIT Nagpur. The work is comprehensive, complete and fit for final evaluation.

Head, Department of Physics
VNIT, Nagpur
Date:

Supervisor,
Dr. Sayandip Ghosh
Assistant Professor
Dept. of Physics, VNIT, Nagpur

Visvesvaraya National Institute of Technology, Nagpur

Non- Plagiarism Certificate

I, **Anup Das**, hereby declare that this dissertation titled **"Floquet Mediated Spin Interaction in Weyl Semimetals"** is carried out by me in the Department of Physics of Visvesvaraya National Institute of Technology, Nagpur. The work is original and has not been submitted earlier whole or in part for the award of any degree/diploma at this or any other Institution / University.

Anup Das
Date:

Dr. Sayandip Ghosh
Assistant Professor
Department of Physics,
VNIT, Nagpur

ORIGINALITY REPORT

5%	4%	2%	0%
SIMILARITY INDEX	INTERNET SOURCES	PUBLICATIONS	STUDENT PAPERS

To Ma, Papa, Didi, Mama and Maha

Acknowledgments

This project would not have been possible without the kind support and help of many individuals and organizations. I would not have progressed in my project without their active direction, assistance, cooperation, and encouragement.

Firstly, I would like to thank my project guide **Dr. Sayandip Ghosh**, Assistant Professor, Department of Physics, VNIT Nagpur, for his continuous support and motivation throughout the project work. It has been a great opportunity for me to work under his guidance on the academic front. I am also grateful for her constant advice, helping nature, and elderly support which made a significant difference in my life.

I am highly thankful to **Dr. B.R. Sankapal**, Head of Department, Department of Physics, VNIT, Nagpur and all my professors for their invaluable cooperation throughout the session.

I am extremely thankful and pay my special honour to **Nikhil Somkule and Abhigya Rangari** (Ph.D. Scholar) for their endless support and dedicated assistance. In every field, either personal or academic, he helped me a lot. His suggested readings and timely guidance made the work easy to understand and manage.

I also would like to thank my project co-partner Mr. Mehboob Alam and Abhishek Dubey (M.Sc. student) for their motive support and sound guidance. They helped me in more ways than one in completing this work.

I would be remiss in not mentioning my parents Mr. Bhuban Chandra Das and Mrs. Dipa Das, my elder sister Dimpy Das and the whole family, who always encouraged me emotionally and financially. They always give me inspiration and hope for doing great in life.

Lastly, I would like to mention my friends and classmates for their cooperation. I am gratefully indebted for their valuable support and understanding.

(Anup Das)

Abstract

This thesis provides a theoretical study of how the RKKY interaction in Weyl Semimetal changes when it is subjected to Floquet driven fields. In order to find the RKKY Hamiltonian, first we calculated the Effective Hamiltonian by incorporating vector potential into the Weyl Hamiltonian. After that, we calculated the real-space Green's function in both momentum and real space using contour integrations. Using this, we calculated the susceptibility. The final expression involves cosine and sine functions that is decaying with distance. This finding provides a detailed insight onto the oscillatory decay nature of the system.

Contents

Contents 4

List of Figures 6

1 Introduction 7

1.1 Weyl Semimetals . . . 7

1.2 RKKY interaction . . . 8

2 RKKY in Dirac Systems 11

2.1 Graphene . . . 11

2.2 Weyl Semimetals . . . 13

3 RKKY in irradiated Dirac System - Graphene 16

3.1 Introduction . . . 16

3.2 Model and Hamiltonian . . . 16

3.2.1 Graphene Dirac Hamiltonian . . . 16

3.2.2 Magnetic Impurities . . . 16

3.2.3 Irradiation and Floquet Hamiltonian . . . 17

3.3 Method: Keldysh-Floquet Green's Functions . . . 17

3.4 Results . . . 17

3.4.1 Undoped Graphene . . . 17

3.4.2 Doped Graphene . . . 18

3.5 Conclusions . . . 18

4 RKKY calculation using Green's Function 19

4.1 Model Hamiltonian . . . 19

4.2 Effective Interaction via Green's Function . . . 19

4.3 Real-Space Green's Function . . . 20

4.4 RKKY Interaction Form . . . 20

5 RKKY in Irradiated Weyl Semimetal **21**
5.1 Formulation 21
5.2 Irradiation 22
5.3 Floquet Hamiltonian 22
5.4 Effective Hamiltonian 23
5.5 Green's function calculation 25
5.6 RKKY Hamiltonian 26
5.7 Susceptibility Calculation 27
5.8 Final Expression 27
5.9 Results 28

6 Summary and Conclusion **29**
6.1 Future Directions 29

Bibliography **31**

List of Figures

1.1 Energy dispersion of a Weyl semimetal around a Weyl node at $k_z = 0$. The conduction and valence bands form a conical structure, touching at the Weyl node. Around the node, the effective band dispersion reads $E(k) = \pm v_F \sqrt{k_x^2 + k_y^2}$. In the figure, we have taken $v_F = 1$. . . 7

1.2 RKKY interaction $J_{RKKY}(r) \propto \cos(2k_F r)/r^3$ as a function of distance r for a metal with Fermi wavevector $k_F = 3.5$. The interaction oscillates between ferromagnetic (red region) ($J > 0$) and antiferromagnetic (blue) ($J < 0$) with a decaying amplitude in metals. 10

2.1 RKKY interaction in graphene. The magnetic impurities are doped at I-th and J-th positions. Symmetry points $\mathbf{K}$ and $\mathbf{K'}$ are also shown. 11

2.2 Distance dependence of the RKKY spin susceptibility $\chi(R)$ in monolayer and bilayer graphene. (a) Monolayer graphene with magnetic impurities on the **same sublattice**: $\chi(R) \propto \frac{1+\cos[(\mathbf{K}-\mathbf{K'})\cdot R]}{R^3}$. (b) Monolayer graphene with impurities on **different sublattices**: $\chi(R) \propto -\frac{1-\cos[(\mathbf{K}-\mathbf{K'})\cdot R-2\theta]}{R^3}$, where θ is the angle between $\mathbf{R}$ and $\mathbf{K}-\mathbf{K'}$. (c) Bilayer graphene with impurities on the **same sublattice**: $\chi(R) \propto \frac{1+\cos[(\mathbf{K}-\mathbf{K'})\cdot R]}{R^2}$. (d) Bilayer graphene with impurities on **different sublattices**: $\chi(R) \propto -\frac{1-\cos[(\mathbf{K}-\mathbf{K'})\cdot R-6\theta]}{R^7}$. These plots demonstrate how sublattice symmetry and interlayer coupling govern the decay and angular dependence of RKKY interaction in graphene-based systems. . 13

Chapter 1

Introduction

1.1 Weyl Semimetals

Weyl semimetals (WSMs) are three-dimensional (3D) analogues of graphene. Its low-energy band structure consists of linearly dispersing bands and these bands cross each other at certain points in momentum space. These points are called Weyl nodes. Weyl nodes act as monopoles of Berry curvature with definite chirality. As for example, if chirality is $+1$, the direction of spin is in the direction of momentum but if chirality is -1 then the direction of spin is in the opposite to momentum [1].

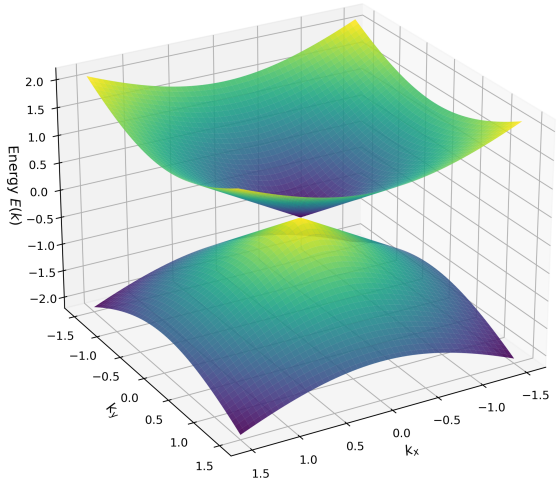

Figure 1.1: Energy dispersion of a Weyl semimetal around a Weyl node at $k_z = 0$. The conduction and valence bands form a conical structure, touching at the Weyl node. Around the node, the effective band dispersion reads $E(k) = \pm v_F \sqrt{k_x^2 + k_y^2}$. In the figure, we have taken $v_F = 1$.

The formation of WSM require breaking of either time-reversal or inversion symmetrry. There are two kind of WSM, namely:
Type-I: It possess point-like Fermi surface at Weyl points.
Type-II: Strongly tilted Weyl cones where Weyl points appear at electron-hole pocket contacts. These family of WSMs are first experimentally confirmed (TaAs, TaP, NbAs, NbP). Non-centrosymmetric crystals with multiple Weyl points. Key observations:

The surface states of WSM shows a highly exotic feature. Every weyl nodes are connected by Weyl fermi arcs. It shows Fermi arcs in ARPES measurements. Fermi arcs are Surface state connections between Weyl points of opposite chirality. Some intersesting transport phenonemons can be seen in Weyl Semimetals. It shows negative longitudinal magnetoresistance(NMLR), optical geometry and planar hall effect. NMLR is used to trace the presence of weyl nodes. Chiral anamoly which is also known as Adler-Bell-Jackiw anomaly, means that the violations of the conservation for number of fermions of different chirality when electric and magnetic field are parallel to each other then pump the weyl fermions between weyl nodes of opposite chirality.

The low-energy Hamiltonian near a Weyl point correspondig to momentum space is given by [2]:

$$H_0(\mathbf{k}) = \chi \left[v_F \boldsymbol{\sigma} \cdot \mathbf{k} + \sigma_0 Q_0 \right] \tag{1.1}$$

where, $\chi = \pm 1$ is the chirality of the Weyl nodes. v_F is the Fermi velocity, $\boldsymbol{\sigma} = (\sigma_x, \sigma_y, \sigma_z)$ are Pauli matrices, $\mathbf{k} = (k_x, k_y, k_z)$ is the crystal momentum which is measured from the Weyl nodes, σ_0 is the 2×2 identity matrix, Q_0 is an energy shift. It represents the tilting or breaking of Lorentz symmetry. It is also known as chiral chemical potential. Some important appplications of Weyl semimetals are in high-speed electronics, spintronics and Quantum computing platforms. It also acts as Topological catalysis.

1.2 RKKY interaction

The **RKKY interaction** (Ruderman-Kittel-Kasuya-Yosida) is an indirect exchange interaction that occurs between magnetic ions or magnetic impurities. This interaction is mediated by the electrons present in the conduction band of the host system. This results in an oscillating magnetic coupling between the ions[3].
Imagine that you have two magnetic ions doped in a sea of free-moving electrons (best source of free electrons is a metal). These ions do not interact directly with

each other. Instead, the interaction between these ions happens as follows:

- **Step 1:** A magnetic ion (having Spin A) polarizes the surrounding conduction electron. This aligns their spins in a certain way.
- **Step 2:** This polarized electron travels through the metal and reaches the second magnetic ion (having spin B).
- **Step 3:** Depending on the distance (r) between the two doped ions, the interaction can be (1.2):
  - **Ferromagnetic**($+ve$) at certain distances.
  - **Antiferromagnetic**($-ve$) at others.

The key point is that the interaction is not constant. Instead. it keeps oscillating with distance. At some separations, the magnets prefer to point in the same direction (ferromagnetic), while at others, they prefer opposite directions (antiferromagnetic). The coupling strength decays with distance. For normal metals, the RKKY inteaction takes the form [4]:

$$J_{\mathrm{RKKY}}(r) \propto \frac{\cos(2k_F r)}{r^3}$$

where k_F is the Fermi wavevector.

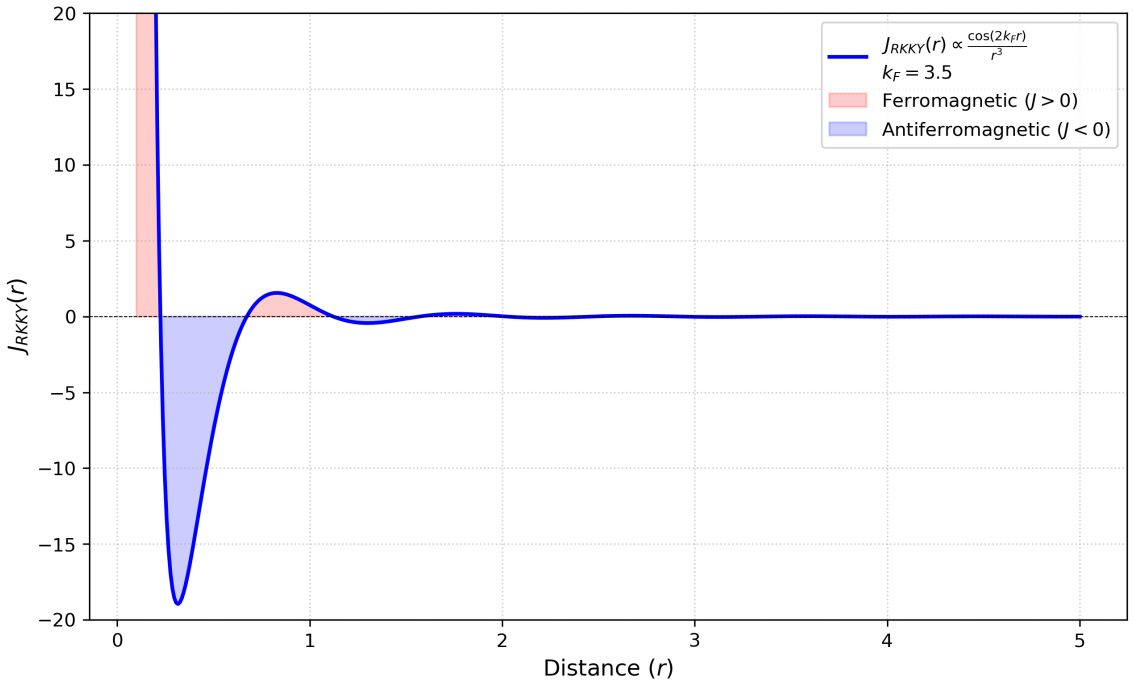

Figure 1.2: RKKY interaction $J_{RKKY}(r) \propto \cos(2k_F r)/r^3$ as a function of distance r for a metal with Fermi wavevector $k_F = 3.5$. The interaction oscillates between ferromagnetic (red region) ($J > 0$) and antiferromagnetic (blue) ($J < 0$) with a decaying amplitude in metals.

Chapter 2

RKKY in Dirac Systems

2.1 Graphene

Graphene has a honeycomb structure. This honeycomb structure is bipartite in nature. Because of this, it exibits symmetry. This symmetry is sub lattice dependent [5]. As mentioned in chapter 1, the RKKY interatcion between two magnetic impurities can be either ferromagnetic or antiferromagnetic depending on their relative positions. In monolayer graphene, when both impurities are doped on the same sublattice (either A-A or B-B), the interaction is ferromagnetic ($+ve$). Also, when the impurities are doped on different sublattices (A-B), the interaction is antiferromagnetic ($-ve$).

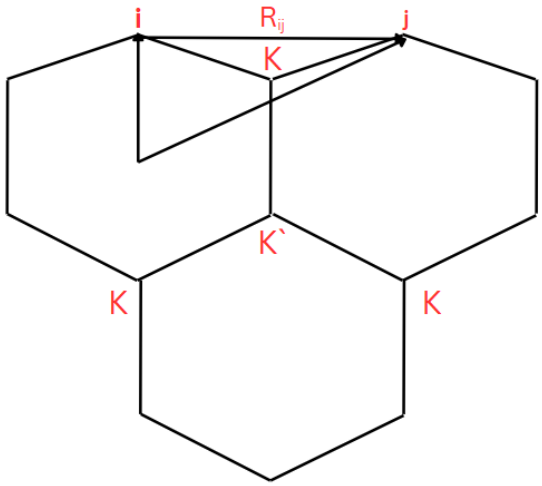

Figure 2.1: RKKY interaction in graphene. The magnetic impurities are doped at I-th and J-th positions. Symmetry points $\mathbf{K}$ and $\mathbf{K}'$ are also shown.

In order to find the RKKY interaction in Graphene, second order perturbation

theory can be used. Using this method, the static spin susceptibility $\chi(\mathbf{R}_{ij})$ in real space can directly be calculated, where $\mathbf{R}_{ij}$ is vector between the impurity sites. If momentum space formulation is done, divergent integrals are obtained.

If J is the interaction strength between the magnetic impurity spin and (mobile) electron's spin, the effective spin interactions between impurities are given as

$$\mathcal{J}_{RKKY} = J^2\chi(\mathbf{R}_{ij}) \tag{2.1}$$

For monolayer graphene, the magnetic spin susceptibility between same-sublattice impurities decays as $1/R^3$. The exact relation reads [6]:

$$\chi^{AA}(\mathbf{R}_{ij}) \propto \frac{1+\cos[(\mathbf{K}-\mathbf{K}')\cdot\mathbf{R}_{ij}]}{R^3}, \tag{2.2}$$

and is shown in Fig. 2.2(a). Here, $R = |\mathbf{R}_{ij}|$.

If the impurities are doped at different sub lattices, the RKKY interaction still decays as $1/R^3$, but also depends on the angle between the vectors $\mathbf{K}-\mathbf{K}'$ and $\mathbf{R}_{ij}$ ($\theta_{\mathbf{R}}$). It reads [6]

$$\chi^{AB}(\mathbf{R}_{ij}) \propto -\frac{1-\cos[(\mathbf{K}-\mathbf{K}')\cdot\mathbf{R}_{ij}-2\theta_{\mathbf{R}}]}{R^3}, \tag{2.3}$$

and is shown in Fig. 2.2(b).

In the case of bilayer graphene, the dispersion relation near the Dirac points is quadratic. Hence, the RKKY interacion decays as $1/R^2$. See Figure 2.2(c). The same-sublattice spin susceptibility is [6]

$$\chi^{AA}(\mathbf{R}_{ij}) \propto \frac{1+\cos[(\mathbf{K}-\mathbf{K}')\cdot\mathbf{R}_{ij}]}{R^2}, \tag{2.4}$$

Furthermore, in the case of substitutional impurities, i.e., where magnetic atoms replace carbon atoms in the lattice, the decay becomes significantly faster. It decays as $1/R^7$ The susceptibility in this case behaves as [6]:

- If doping is done at same sub lattice See Figure (2.2)(c)

$$\chi^{S_AS_A}(\mathbf{R}_{ij}) \propto \frac{1+\cos[(\mathbf{K}-\mathbf{K}')\cdot\mathbf{R}_{ij}]}{R^7} \tag{2.5}$$

- If doping is done at different sub lattice, See Figure (2.2)(d)

$$\chi^{S_AS_B}(\mathbf{R}_{ij}) \propto -\frac{1-\cos[(\mathbf{K}-\mathbf{K}')\cdot\mathbf{R}_{ij}-6\theta_{\mathbf{R}}]}{R^7} \tag{2.6}$$

These findings have important applications for the design of graphene-based spintronic devices, where control over magnetic coupling is essential. However, there are also certain limitations. While doing the entire calculation, it is assumed that electrons are non-interacting and a simplified two-impurity scenario. Practically it is impossible to dope only two impurities in a system and also, electrons may interact among themselves. These assumptions could lead to discrepancies when applying the theoretical results to practical systems.

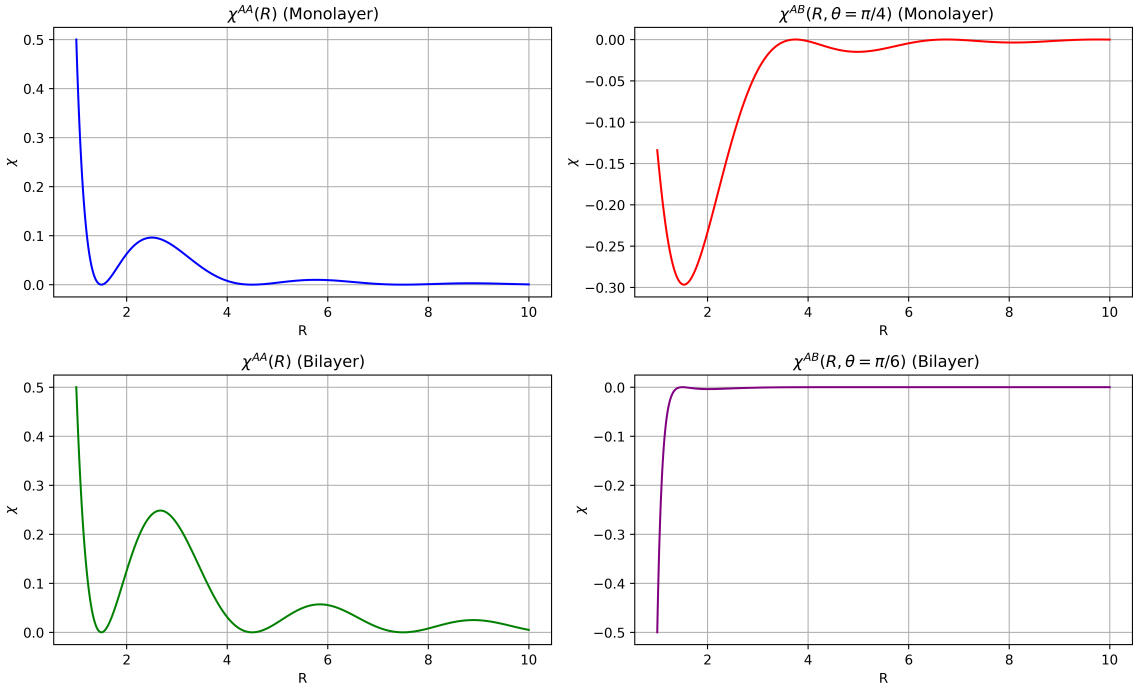

Figure 2.2: Distance dependence of the RKKY spin susceptibility $\chi(R)$ in monolayer and bilayer graphene. (a) Monolayer graphene with magnetic impurities on the **same sublattice**: $\chi(R) \propto \frac{1+\cos[(\mathbf{K}-\mathbf{K}')\cdot R]}{R^3}$. (b) Monolayer graphene with impurities on **different sublattices**: $\chi(R) \propto -\frac{1-\cos[(\mathbf{K}-\mathbf{K}')\cdot R-2\theta]}{R^3}$, where θ is the angle between $\mathbf{R}$ and $\mathbf{K}-\mathbf{K}'$. (c) Bilayer graphene with impurities on the **same sublattice**: $\chi(R) \propto \frac{1+\cos[(\mathbf{K}-\mathbf{K}')\cdot R]}{R^2}$. (d) Bilayer graphene with impurities on **different sublattices**: $\chi(R) \propto -\frac{1-\cos[(\mathbf{K}-\mathbf{K}')\cdot R-6\theta]}{R^7}$. These plots demonstrate how sublattice symmetry and interlayer coupling govern the decay and angular dependence of RKKY interaction in graphene-based systems.

2.2 Weyl Semimetals

Now we consider two localized impurities having spin S_1 and S_2 embedded in 3D Weyl semimetallic system having electronic Hamiltonian $H_{\text{el}} = v_0(\sigma_x k_x + \sigma_y k_y + \chi\sigma_z k_z)$.

The indirect exchange interaction between those localized impurities Weyl fermions is described by the effective RKKY Hamiltonian [7]:

$$H_{\mathrm{RKKY}} = F_1 \mathbf{S}_1 \cdot \mathbf{S}_2 + F_2 \hat{\rho} \cdot (\mathbf{S}_1 \times \mathbf{S}_2) + F_3 (\mathbf{S}_1 \cdot \hat{\rho})(\mathbf{S}_2 \cdot \hat{\rho}) + F_4 S_1^z S_2^z \tag{2.7}$$

where the functions F_1, F_2, F_3 and F_4 are given by :

$$\begin{aligned} F_1 &= -\frac{8\pi^3 J^2}{\Omega_{BZ}^2 v_o R^5} I_1 \\ F_2 &= -\frac{64\pi^3 J^2}{\Omega_{BZ}^2 v_o R^5} I_2 \\ F_3 &= -\frac{16\pi^3 J^2}{\Omega_{BZ}^2 v_o R^5} I_3 \\ F_4 &= -\frac{16\pi^3 J^2}{\Omega_{BZ}^2 v_o R^5} I_4 \end{aligned} \tag{2.8}$$

I_1, I_2, I_3, I_4 are dimensionless couplings defined as:

$$I_1 = \cos^2(Qz) \left\{ (1 - 2\gamma^2)\cos(2\gamma) + 2\gamma \sin(2\gamma) + \left[\sin^2(\theta_R) + W^2\right] I_0 \right\} \tag{2.9}$$

$$I_2 = \cos^2(Qz) \left[\gamma \cos(2\gamma) + (\gamma^2 - 1)\cos(\gamma)\sin(\gamma) \right] \tag{2.10}$$

$$I_3 = \cos^2(Qz) I_0 \tag{2.11}$$

$$I_4 = \sin^2(Qz)\cos^2(\theta_R) I_0 \tag{2.12}$$

where, $I_0 = (5 - 2\gamma^2)\cos(2\gamma) + 6\gamma \sin(2\gamma)$, $\gamma = \frac{R\epsilon_F}{v_0}$.. Here, Ω_{BZ} is the volume of first Brillouin zone, $z = R\cos(\theta_{\mathrm{R}})$, $W = \tan(Qz)\cos(\theta_{\mathrm{R}})$, with the Weyl nodes located at $(0, 0, \pm Q)$, and ϵ_F the Fermi energy, θ_{R} the azimuthal angle of $\mathbf{R}_{ij}$. Now, let us analyze these terms

- $F_1 \mathbf{S}_1 \cdot \mathbf{S}_2$: It means Heisenberg-type interaction. It represents the direct exchange coupling between the two spins. It tends to align the spins parallel (ferromagnetic) or antiparallel (antiferromagnetic) depending on the sign of F_1. Imazine two bar magnets either sticking together or repelling based on the orientation of their poles.

- $F_2 \hat{\rho} \cdot (\mathbf{S}_1 \times \mathbf{S}_2)$: This type of spin arrangement is called Dzyaloshinskii-Moriya (DM) interaction. It arises because of the presence of spin-orbit Coupling. Because of DM interaction, a twisting or chiral arrangement is induced between the two spins

- $F_3 (\mathbf{S}_1 \cdot \hat{\rho})(\mathbf{S}_2 \cdot \hat{\rho})$: This term represents an anisotropic interaction in which the coupling depends on the projection of the spins along the unit vector $\hat{\rho}$

connecting them.

- $F_4 S_1^z S_2^z$: This is an Ising-type interaction along the z-axis. It involves only the z-th component of the spins. It is relevant in systems where spins prefer to align along a particular axis. This term cares only whether the spins point up or down, and acts to align or oppose them in that direction.

These results were derived using a real-space Green's function approach applied to a two-band model of Weyl fermions, employing second-order perturbation theory in the exchange coupling J, along with spherical harmonic expansion of the Green's function.

At the Weyl node ($\epsilon_F = 0$), all of the above terms decay as R^{-5}. But for finite Fermi energy, the decay slows to R^{-3}. The interference that occurs between contributions from distinct Weyl nodes leads to a characteristic beating pattern. Angularly, the DM interaction lies in the plane perpendicular to the Weyl node separation. The Ising component on the other hand vanishes in that plane and the Heisenberg term shows the most significant angular adjustment. These results are very important and has application in spintronics, particularly in how topology influences magnetic behavior. Comparatively, the RKKY interaction in WSMs decays faster (R^{-5}) than in graphene (R^{-3}) or a 2D electron gas (R^{-2}), and exhibits more intricate angular dependence due to the 3D structure and Weyl node separation.

Chapter 3

RKKY in irradiated Dirac System - Graphene

3.1 Introduction

Now we study the effect of a time-periodic driving field (circularly polarized light) in the RKKY interaction for Graphene as carried out in Ref. [8].

In absence of irradiation, owing to its Dirac cone dispersion:

- for **undoped** graphene, RKKY decays as $1/R^3$.
- for **doped** graphene, RKKY decays as $1/R^2$ and oscillates with period π/k_F.

3.2 Model and Hamiltonian

3.2.1 Graphene Dirac Hamiltonian

The low-energy electrons in graphene are described by:

$$H_0 = \hbar v_F(\tau\sigma_x k_x + \sigma_y k_y), \tag{3.1}$$

where v_F is the Fermi velocity and $\tau = \pm 1$ distinguishes the K and K' valleys.

3.2.2 Magnetic Impurities

Magnetic impurities couple locally to electron spins:

$$H_{\text{imp}} = \lambda\delta(\boldsymbol{r})\boldsymbol{S}\cdot\boldsymbol{S}_1 + \lambda\delta(\boldsymbol{r}-\boldsymbol{R})\boldsymbol{S}\cdot\boldsymbol{S}_2. \tag{3.2}$$

3.2.3 Irradiation and Floquet Hamiltonian

Under irradiation with circularly polarized light:

$$\boldsymbol{E}(t) = E_0 \left[\cos(\Omega t)\hat{x} + \sin(\Omega t)\hat{y}\right], \tag{3.3}$$

the time-dependent Hamiltonian becomes:

$$H(t) = \hbar v_F(\tau\sigma_x k_x + \sigma_y k_y) - A\tau\sigma_x \sin(\Omega t) + A\sigma_y \cos(\Omega t), \tag{3.4}$$

with $A = v_F e E_0/\sqrt{2}\Omega$.

Using Floquet theory, the system develops a light-induced bandgap Δ at the Dirac points:

$$\Delta \propto \frac{A^2}{\hbar\Omega}. \tag{3.5}$$

3.3 Method: Keldysh-Floquet Green's Functions

The RKKY interaction energy is given by:

$$E_{\mathrm{RKKY}}(\boldsymbol{R}) = J(\boldsymbol{R})\, \boldsymbol{S}_1 \cdot \boldsymbol{S}_2, \tag{3.6}$$

where the coupling constant is:

$$J(\boldsymbol{R}) = \lambda^2\hbar^2 \int_{-\hbar\Omega/2}^{\hbar\Omega/2} \frac{d\bar{\Omega}}{2\pi} \operatorname{Im}\left\{\operatorname{Tr}\left[G^R_{\alpha\beta}(\boldsymbol{R},\bar{\Omega})G^<_{\beta\alpha}(-\boldsymbol{R},\bar{\Omega})\right]\right\}. \tag{3.7}$$

In the weak driving regime ($A/\hbar\Omega \ll 1$), the F_0 approximation is used:

- Only zero-photon processes are kept.
- The Hamiltonian becomes block-diagonal.
- The quasienergy spectrum is gapped and the Fermi velocity is renormalized.

Green's functions in the real space are obtained analytically using Hankel functions $H_0^{(1)}$ and $H_1^{(1)}$.

3.4 Results

3.4.1 Undoped Graphene

For $E_F = 0$:

- In equilibrium (no light): $J(R) \propto 1/R^3$ (ferromagnetic).
- Under irradiation:
  - RKKY magnitude decreases with increasing light intensity.
  - A new term $\propto 1/R$ appears.
  - RKKY coupling can flip sign (FM $\rightarrow$ AFM) depending on parameters.

Analytical formula:

$$J(R) \sim -F_0^2 \frac{1}{R^3}(1 + \cos(2\boldsymbol{K} \cdot \boldsymbol{R})) + \frac{1}{R} \times (\text{light-induced correction}). \tag{3.8}$$

3.4.2 Doped Graphene

For $E_F \neq 0$:

- In equilibrium: $J(R)$ oscillates with period π/k_F.
- Under irradiation:
  - The effective Fermi momentum k_F decreases as the light-induced gap increases.
  - The oscillation period increases with the intensity of the light.
  - Strong enough driving can cause the behavior to cross over to undoped-like RKKY.

Asymptotic behavior for $k_F R \gg 1$:

$$J(R) \sim \frac{\cos(2k_F R)}{R^2} + \text{light-induced corrections}. \tag{3.9}$$

3.5 Conclusions

The RKKY interaction in graphene can be dynamically tuned by optical driving:

- Change the magnitude.
- Modify the oscillation period.
- Flip the sign of interaction (FM to AFM).

This offers a pathway to **optically control magnetic interactions** for future **spintronics** and **quantum information** applications.

Chapter 4

RKKY calculation using Green's Function

4.1 Model Hamiltonian

We consider two localized magnetic moments $\mathbf{S}_1$ and $\mathbf{S}_2$ interacting with conduction electrons through an *s-d* exchange interaction. The total Hamiltonian is

$$H = H_0 + H_{\text{int}}, \tag{4.1}$$

where

$$H_0 = \sum_{\mathbf{k},\sigma} \epsilon_{\mathbf{k}}\, c^{\dagger}_{\mathbf{k}\sigma} c_{\mathbf{k}\sigma}, \tag{4.2}$$

$$H_{\text{int}} = -J \sum_{i=1}^{2} \mathbf{S}_i \cdot \mathbf{s}(\mathbf{R}_i), \tag{4.3}$$

with H_0 is the electronic Hamiltonian and H_{int} is the interaction between impurity spin and mobile electrons. The conduction electron spin density operator is

$$\mathbf{s}(\mathbf{R}_i) = \frac{1}{2} c^{\dagger}_{\alpha}(\mathbf{R}_i)\, \boldsymbol{\sigma}_{\alpha\beta}\, c_{\beta}(\mathbf{R}_i), \tag{4.4}$$

with $\boldsymbol{\sigma}$ being the vector of Pauli matrices.

4.2 Effective Interaction via Green's Function

The indirect exchange interaction between $\mathbf{S}_1$ and $\mathbf{S}_2$ mediated by the conduction electrons can be obtained by computing the energy correction due to H_{int} to all orders

in J, using the electron Green's function.

The effective Hamiltonian can be written as:

$$H_{\text{eff}} = \frac{J^2}{4} \sum_{i,j} S_1^i S_2^j \, \chi^{ij}(\mathbf{R}), \tag{4.5}$$

where $\mathbf{R} = \mathbf{R}_1 - \mathbf{R}_2$ and $\chi^{ij}(\mathbf{R})$ is the real-space static spin susceptibility defined via the electron Green's functions as:

$$\chi^{ij}(\mathbf{R}) = -i \int_{-\infty}^{\infty} \frac{d\omega}{2\pi} \, \text{Tr} \left[\sigma^i G(\mathbf{R}, \omega + i0^+) \, \sigma^j G(-\mathbf{R}, \omega + i0^+) \right] f(\omega), \tag{4.6}$$

where $f(\omega)$ is the Fermi-Dirac distribution and $G(\mathbf{R}, \omega)$ is the electron Green's function in real space.

4.3 Real-Space Green's Function

The non-interacting Green's function in real space is given by

$$G(\mathbf{R}, \omega) = \int \frac{d^3k}{(2\pi)^3} \, \frac{e^{i\mathbf{k}\cdot\mathbf{R}}}{\omega - \epsilon_{\mathbf{k}} + i0^+}. \tag{4.7}$$

For an isotropic free electron dispersion $\epsilon_{\mathbf{k}} = \frac{\hbar^2 k^2}{2m}$, this integral can be evaluated explicitly, and at zero temperature $T = 0$, the susceptibility simplifies due to the step function nature of $f(\omega)$.

4.4 RKKY Interaction Form

In an isotropic system and at $T = 0$, the Green's functions yield a scalar susceptibility after spin trace, leading to the effective Heisenberg-type interaction:

$$H_{\text{RKKY}} = J_{\text{RKKY}}(R) \, \mathbf{S}_1 \cdot \mathbf{S}_2, \tag{4.8}$$

with

$$J_{\text{RKKY}}(R) = -\frac{J^2}{\pi} \Im \int_{-\infty}^{\infty} d\omega \, f(\omega) \left[G(\mathbf{R}, \omega + i0^+) \right]^2. \tag{4.9}$$

Chapter 5

RKKY in Irradiated Weyl Semimetal

5.1 Formulation

Let us consider a 3D Weyl Semimetal with a pair of Weyl points. It is separated in the Brillouin zone which contains two magnetic impurities In order to keep the linearly dispersing bands, the strength of the impurities is assumed to be small. The Hamiltonian describing the Weyl Fermions is given by [7]

$$H_0 = \chi \left[v_F \boldsymbol{\sigma} \cdot (\mathbf{k} - \chi \mathbf{Q}) + \sigma_0 Q_0 \right] \tag{5.1}$$

where

- $\mathbf{k}$ is the wave vector, $\mathbf{k} = \dfrac{2\pi}{\lambda}$,
- v_F is the Fermi velocity, $v_F = 10^6\,\mathrm{m/s}$,
- $\chi = \pm 1$ denotes the chirality of the Weyl nodes,
- $\boldsymbol{\sigma}$ represents the Pauli matrices,
- σ_0 is the identity matrix,
- $\mathbf{Q}$ and Q_0 are parameters related to node separation in momentum and energy.

If $Q = Q_o = 0$ the weyl nodes overlap. In such case, the Hamiltonian obtained is the Dirac Hamiltonian. For a non-centro symmetric system that also preserves Time Reversal Symmetry(TRS), [9] $Q = 0$ and $Q_o \neq 0$. Therefore, the Weyl nodes were located at the same $\mathbf{K}$ point but at different energies if the TRS is broken, but the

system has inversion symmetry;$Q \neq 0$ and $Q_o = 0$. That is, the Weyl nodes have the same energy but different $\mathbf{K}$ points. For broken TRS, (5.1) takes the form

$$H_0 = \chi \left[v_F \boldsymbol{\sigma} \cdot \mathbf{k} + \sigma_0 Q_0 \right] \tag{5.2}$$

5.2 Irradiation

We consider normal incidence of a circularly polarized (CP) light on the Weyl semimetal. The electric field is given by [10]

$$\mathbf{E}(t) = \frac{E_0}{\sqrt{2}} \left[\cos(\Omega t)\, \hat{\mathbf{x}} + \sin(\Omega t)\, \hat{\mathbf{y}} \right], \tag{5.3}$$

where E_0 is the field amplitude and Ω is the frequency of the light.

The electromagnetic field couples to the Weyl Hamiltonian via the minimal coupling scheme [11]

$$\mathbf{k} \to \mathbf{k} + e\mathbf{A}(t), \tag{5.4}$$

where $\mathbf{A}(t)$ is the vector potential related to the electric field by [12]

$$\mathbf{E}(t) = -\frac{\partial \mathbf{A}(t)}{\partial t} + \nabla \phi \tag{5.5}$$

Assuming the scalar potential $\phi = 0$, this simplifies to

$$\mathbf{E}(t) = -\frac{\partial \mathbf{A}(t)}{\partial t} \quad \Rightarrow \quad \mathbf{A}(t) = -\int \mathbf{E}(t)\, dt \tag{5.6}$$

We include vector potential because it ensures that the Hamiltonian is gauge-invariant. If we incorporate (5.3) directly into (5.1), we would have neglected the magnetic contribution of the Electro magnetic field. Upon solving (5.6), we get

$$\mathbf{A}(t) = -\frac{E_0}{\sqrt{2}\,\Omega} \left[\sin(\Omega t)\, \hat{\mathbf{x}} - \cos(\Omega t)\, \hat{\mathbf{y}} \right]. \tag{5.7}$$

5.3 Floquet Hamiltonian

The resulting time dependent irradiated Hamiltonian of the WSM is [6]

$$H_{irr}(t) = H_0 + \chi \left[v_F \boldsymbol{\sigma} \cdot (\mathbf{k} - e\mathbf{A}) \right] - v_F \boldsymbol{\sigma} \cdot \mathbf{Q} \tag{5.8}$$

Using the explicit form of H_0 from (5.1) and $\mathbf{A}(t)$ from (5.6), this becomes

$$H_{\text{irr}}(t) = H_0 - Cv_F\left[\sin(\Omega t)\,(\boldsymbol{\sigma}\cdot\mathbf{k})\,\hat{\mathbf{x}} - \cos(\Omega t)\,(\boldsymbol{\sigma}\cdot\mathbf{k})\,\hat{\mathbf{y}}\right] - C\sigma_0 Q_0\left[\sin(\Omega t)\,\hat{\mathbf{x}} - \cos(\Omega t)\,\hat{\mathbf{y}}\right] \tag{5.9}$$

where $C = \dfrac{\chi v_F E_o}{\sqrt{2}}$.
Since $H_{\text{irr}}(t)$ is subjected to a Floquet-driven field, it becomes a periodic function of time, i.e.,

$$H_{\text{irr}}(t) = H_{\text{irr}}(t+T),$$

where $T = \dfrac{2\pi}{\Omega}$ is the period of the drive.

The Floquet Hamiltonian is defined in the Fourier space as

$$H_{F,mn} = H_{mn} - n\hbar\Omega\delta_{mn}, \tag{5.10}$$

where H_{mn} is the floquet matrix [13]-[14] given by

$$H_{mn} = \frac{1}{T}\int_0^T e^{i(m-n)\Omega t} H_{\text{irr}}(t)dt$$

$$\implies H_{mn} = (H_0 - v_F\,\boldsymbol{\sigma}\cdot\mathbf{Q})\,\delta_{m,n} + \left(\frac{C}{2}(-i\sigma_x + \sigma_y)\right)\delta_{m,n-1} - \left(\frac{C}{2}(i\sigma_x + \sigma_y)\right)\delta_{m,n+1}. \tag{5.11}$$

5.4 Effective Hamiltonian

In the regime of high-frequency, off-resonant light irradiation, we can use the Van-Vleck perturbation theory to expand the full Floquet Hamiltonian matrix in powers of $\dfrac{1}{\Omega}$ into a finite-dimensional effective Hamiltonian [15], [16]. The Van- Vleck perturbation theory is effected by applying a unitary transformation in order to construct an effective Hamiltonian using the degenerate perturbation theory [17]. The effective Hamiltonian is written in the form of the following series:

$$H_{\text{eff}} = \sum_{n=0}^{\infty} {H_{vv}}^n = H_{vv}^{(0)} + H_{vv}^{(}1) + H_{vv}^{(2)} + \cdots \tag{5.12}$$

The first few terms in the expansion are given by:

- **Zeroth-order term (time-averaged Hamiltonian):**

$$H_{vv}^{(0)} = 0$$

- **First-order term (commutator of virtual photon processes):**

$$H_{vv}^{(1)} = H_o \text{(5.1)}$$

- **Second-order term (nested commutators):**

$$H_{vv}^{(2)} = \frac{[H_-(k), H_+(k)]}{\hbar\Omega}$$

Here, H_n are the Fourier components of the time-periodic Hamiltonian $H_{\text{irr}}(t)$, defined as:

$$H_\pm(k) = \frac{1}{T}\int_0^T H_{\text{irr}}(k)\, e^{\mp i\Omega t}\, dt \tag{5.13}$$

Substituting the form of $H_{\text{irr}}(t)$ from (5.9), and expressing sine and cosine in exponential form

$$H_-(k) = \frac{1}{T}\int_0^T e^{+i\Omega t}\left[H_0 - \frac{Cv_F}{2i}\left(e^{i\Omega t} - e^{-i\Omega t}\right)\sigma_x + \frac{C}{2}\left(e^{i\Omega t} + e^{-i\Omega t}\right)\sigma_y - v_F\boldsymbol{\sigma}\cdot\mathbf{Q}\right]dt$$
$$H_+(k) = \frac{1}{T}\int_0^T e^{-i\Omega t}\left[H_0 - \frac{Cv_F}{2i}\left(e^{i\Omega t} - e^{-i\Omega t}\right)\sigma_x + \frac{C}{2}\left(e^{i\Omega t} + e^{-i\Omega t}\right)\sigma_y - v_F\boldsymbol{\sigma}\cdot\mathbf{Q}\right]dt \tag{5.14}$$

Upon Solving the integration, we get

$$H_\pm(k) = \frac{C}{2}(\sigma_y \mp i\sigma_x). \tag{5.15}$$

Therefore, $[H_-, H_+] = -C^2\sigma_z$. Hence the effective hamiltonian (5.12) upto the second term is

$$H_{eff} = H_0 - \frac{v_f^2 E_o^2}{2\hbar\Omega}\sigma_z = H_0 - D^2\sigma_z, \tag{5.16}$$

where $D = \dfrac{v_f^2 E_o^2}{2\hbar\Omega}$.

The eigenvalues of H_{eff} is

$$E_\pm = \chi v_F\sqrt{k_x^2 + k_y^2 + (k_z - \chi\frac{v_F E_o^2}{2\hbar\Omega})^2} = \chi v_f\tilde{k} \tag{5.17}$$

where $\tilde{k} = \sqrt{k_x^2 + k_y^2 + (k_z - \Delta^2)}$ and $\Delta = (\dfrac{v_F E_o^2}{2\hbar\Omega})^2$. The corresponding eigenvectors are

$$|k, \mp\rangle = \begin{pmatrix} \dfrac{(\Delta - k_z v_F) \pm \sqrt{\Delta^2 + 2\Delta k_z v_F + v_F^2 k^2}}{v_F(k_x + ik_y)} \\ 1 \end{pmatrix} \tag{5.18}$$

5.5 Green's function calculation

The momemntum-space Green's function is now calculated and reads

$$G(\mathbf{k}, i\omega_n) = \frac{i\omega_n + \chi v_F\, \boldsymbol{\sigma}\cdot\mathbf{k} - D^2\sigma_z}{(i\omega_n)^2 - (D^2 - 2Dk_z v_F + \epsilon_k^2)} \tag{5.19}$$

where $\epsilon_k^2 = \pm v_F^2 k^2$. Here, ω_n is the Fermionic Matsubara frequency. In the low-temperature limit, taking analytical continuation $i\omega_n \longrightarrow \epsilon + i\eta$ (η being positive infinitesimal) and Fourier transforming into coordinate space, we get

$$G_\chi(\pm\mathbf{R}, \epsilon) = \int \frac{d^3\tilde{k}}{(2\pi)^3}\, \frac{\epsilon\sigma_o \pm v_F\, \boldsymbol{\sigma}\cdot\tilde{\mathbf{k}}}{(\epsilon - i\eta)^2 - \epsilon_k^2} \exp(i\mathbf{k}\cdot\mathbf{R}) \exp(-\Delta) \tag{5.20}$$

where $\varepsilon_k = \pm v_F \tilde{k}$. In general, the momentum $\mathbf{k}$ can be resolved into the directions parallel and perpendicular to $\mathbf{e}_R$ as:

$$\mathbf{k} = \mathbf{k}_\parallel + \mathbf{k}_\perp \equiv (\mathbf{k}\cdot\mathbf{e}_R)\mathbf{e}_R + (\mathbf{e}_R \times \mathbf{k}) \times \mathbf{e}_R \quad \text{with} \quad \mathbf{e}_R = \mathbf{R}/|\mathbf{R}|.$$

Now (5.20) is written as

$$\begin{aligned} G_\chi(\pm\mathbf{R}, \epsilon) &= \int \frac{d^3\tilde{k}}{(2\pi)^3}\, \frac{\epsilon\sigma_0}{(\epsilon + i\eta)^2 - \epsilon_k^2} \exp(ikR\cos\theta) \exp(-\Delta) \\ &\quad \pm \int \frac{d^3\tilde{k}}{(2\pi)^3}\, \frac{v_F\, \boldsymbol{\sigma}\cdot\tilde{\mathbf{k}}}{(\epsilon + i\eta)^2 - \epsilon_k^2} \exp(ikR\cos\theta) \exp(-\Delta) \qquad (5.21) \\ &= \sigma_o G_o(R;\epsilon) \pm \chi\boldsymbol{\sigma}\cdot\mathbf{e}_R G_R(R;\epsilon) \qquad (5.22) \end{aligned}$$

Here,

$$\begin{aligned} G_0(R;\varepsilon) &= \varepsilon \int \frac{d^3\tilde{\mathbf{k}}}{(2\pi)^3} \frac{\exp(i\tilde{k}R\cos\theta)}{(\varepsilon + i\eta)^2 - v_F^2\tilde{k}^2} \\ &= -\frac{\varepsilon}{4\pi^2 v_F^2} \int_0^\infty \frac{\tilde{k}^2 d\tilde{k}}{\tilde{k}^2 - (\varepsilon + i\eta)^2/v_F^2} \int_0^\pi \sin\theta \exp(i\tilde{k}R\cos\theta) d\theta \end{aligned} \tag{5.23}$$

where θ is the angle between vector $\tilde{\mathbf{k}}$ and vector $\mathbf{R}$. Integrating over θ leads to

$$G_0(R;\varepsilon) = -\frac{\varepsilon}{i4\pi v_F^2 R} \int_0^\infty \frac{\tilde{k}\left[\exp(i\tilde{k}R) - \exp(-i\tilde{k}R)\right] d\tilde{k}}{\tilde{k}^2 - (\varepsilon + i\eta)^2/v_F^2}. \tag{5.24}$$

Due to the symmetry of the integrand of $\tilde{k}$, the integration of $G_0(R;\varepsilon)$ can be recast as:

$$G_0(R;\varepsilon) = -\frac{\varepsilon}{i4\pi v_F^2 R}\int_{-\infty}^{\infty}\frac{\tilde{k}\exp(i\tilde{k}R)\,d\tilde{k}}{\tilde{k}^2-(\varepsilon+i\eta)^2/v_F^2}. \tag{5.25}$$

Also,

$$G_R(R;\epsilon) = -i\frac{v_f}{\epsilon}\frac{\partial G_o(R;\epsilon)}{\partial x} \tag{5.26}$$

After carrying out the contour integration, it gives

$$G_o(R;\epsilon) = -\frac{1}{4\pi v_f R^2} \tag{5.27}$$

Solving this two integrals gives:

$$\begin{aligned} G_\chi(\pm\mathbf{R},\epsilon) = -\sigma_0\frac{1}{4\pi v_f R^2}\left(\frac{\epsilon R}{v_f}-\Delta\right)\exp\left(\frac{\epsilon R}{v_f}-\Delta\right) \\ \pm\left[\frac{1}{4\pi v_f R^3}\left(\frac{\epsilon R}{v_f}-\Delta\right)\exp\left(\frac{\epsilon R}{v_f}-\Delta\right)-\frac{\epsilon}{v_f}\cdot\frac{1}{4\pi v_f R^2}\left(1+\frac{\epsilon R}{v_f}-\Delta\right)\right] \end{aligned} \tag{5.28}$$

Now, define:

$$\xi = \frac{\epsilon R}{v_f}-\Delta$$

Then the Green's function in the real space from equation (5.22) is:

$$\begin{aligned} G_\chi(\pm\mathbf{R},\epsilon) = -\sigma_0\frac{1}{4\pi v_f R^2}\,\xi\,e^{\xi} \\ \pm\,\chi\boldsymbol{\sigma}\cdot\boldsymbol{e_R}\left[\frac{1}{4\pi v_f R^3}\,\xi\,e^{\xi}-\frac{\epsilon}{v_f}\cdot\frac{1}{4\pi v_f R^2}\,(1+\xi)\right] \end{aligned} \tag{5.29}$$

As we can see, the function has two terms: the first term corresponds to the non-interacting system and the second term depends on the energy ϵ. It carries the interaction effect.

5.6 RKKY Hamiltonian

If S_1^α and S_2^β are the two spin components of the impurities,then the RKKY Hamiltonian is given as:

$$H_{\text{RKKY}} = -J^2\sum_{\alpha,\beta}S_1^\alpha S_2^\beta\chi_{\alpha\beta}(R), \tag{5.30}$$

where $\chi_{\alpha\beta}(R)$ is the spin susceptibility given by:

$$\chi_{\alpha\beta}(R) = -\frac{1}{\pi}\text{Im}\int_{-\infty}^{\epsilon_F}d\epsilon\,\text{Tr}\left[\sigma_\alpha G(R,\epsilon^+)\sigma_\beta G(-R,\epsilon^+)\right]. \tag{5.31}$$

5.7 Susceptibility Calculation

Using the Green's functions obtained at equation(5.29) $G(R,\epsilon)$, at first, the product of $G(R,\epsilon)$ and $G(-R,\epsilon)$ is calculated. We expanded this product to leading order in $1/R$. This approximation preserves the leading order terms that contributes to the susceptibility.:

$$G(R,\epsilon)G(-R,\epsilon) \approx \left(\frac{1}{4\pi v_f R^2}\right)^2 \xi^2 e^{2\xi}\left[\sigma_0 - (R\cdot\sigma)^2 + O\left(\frac{1}{R}\right)\right]. \tag{5.32}$$

where, $O\left(\frac{1}{R}\right)$ includes higher-ordered terms that decreases more faster with distance and the contributions are negligible at very large values of R.

We know,

$$\mathrm{Tr}[\sigma_\alpha\sigma_0\sigma_\beta\sigma_0] = 2\delta_{\alpha\beta}, \tag{5.33}$$

and

$$\sigma_\alpha \mathrm{Tr}[(R\cdot\sigma)\sigma_\beta(R\cdot\sigma)] = 2\left[2(R^\alpha R^\beta) - \delta_{\alpha\beta}\right]. \tag{5.34}$$

Thus,

$$\mathrm{Tr}[G(R,\epsilon^+)\sigma_\alpha G(-R,\epsilon^+)\sigma_\beta] = \frac{1}{16\pi^2 v_f^2 R^4}\xi^2 \exp^{2\xi}\left[2\delta_{\alpha\beta} - 4(R^\alpha R^\beta)\right] + O\left(\frac{1}{R^5}\right). \tag{5.35}$$

The final expression for $\chi(R)$ is calculated to be:

$$\chi(R) \sim \frac{J^2}{v_f}\cos(2k_F R)\,(k_F R)^3\left[\mathbf{S_1}\cdot\mathbf{S_2} - 3(\mathbf{S_1}\cdot\mathbf{R})(\mathbf{S_2}\cdot\mathbf{R})\right]. \tag{5.36}$$

5.8 Final Expression

The spin susceptibility is integrated over energy The resulting Hamiltonian for the RKKY interaction is:

$$\begin{aligned} H_{\mathrm{RKKY}} \approx{}& \frac{J^2\epsilon_F}{4\pi^2 v_f^2}\left[(k_F R)^{-4}\sin(2k_F R) - 2(k_F R)^{-2}\cos(2k_F R)\right]\,\mathbf{S_1}\cdot\mathbf{S_2} \\ &+ \frac{J^2\epsilon_F}{4\pi^2 v_f^2}\left[3\left(2k_F R\cos(2k_F R) - \sin(2k_F R)\right)\right](k_F R)^{-4}\,(\mathbf{S_1}\cdot\mathbf{R})(\mathbf{S_2}\cdot\mathbf{R}). \end{aligned} \tag{5.37}$$

5.9 Results

Because of $\sin(2k_F R)$ and $\cos(2k_F R)$ terms, the interaction is clearly an oscillatorty function of R. Also, $\sin(2k_F R)$ and $\cos(2k_F R)$ decays with R as R^{-4} and R^{-2} respectively. Because of the involvment of $(\mathbf{S_1} \cdot \mathbf{R})(\mathbf{S_2} \cdot \mathbf{R})$ it is clear that the interaction is also anisotropic in nature.

Chapter 6

Summary and Conclusion

The aim of this research is to calculate the RKKY interaction when an Weyl Semimetal is subjected to Floquet driven fields. Based on the calculations, it is observed that the the RKKY interaction for Weyl semimetals is also an oscillatory decay function with respect to the distance. When a Floquet driven field, or simply a circularly polarized light is irradiated on an Weyl semimetal, then the vector potential associated with the light couples with the Weyl Hamiltonian via minimal coupling scheme. Since the irradiated light is a periodic function of time, therefore the Hamiltonian of the Weyl semimetal also becomes a periodic. Assuming that the frequency of the irradiated light is very much greater than the inherent frequency, we used the Van Planck Perturbation theory to expand the Hamiltonian in the inverse power of frequency of the incident circularly polarised light. We only expanded upto the first order. The higher order terms are neglected. The, using this effective Hamiltonian, we first calculated the Green's Function in the momentum space. After doing a fourier transformation of this Green's function, the Real Space's Green function is obtained. The susceptibility is calculated using this Green's Function. After calculating the susceptibility, it is integrated over energy within limits to calculate the RKKY interaction. We found that the interaction is a combined function of sine and cosine and it is decaying as powers of R^{-4} and R^{-2}.

6.1 Future Directions

- We calculated the RKKY interaction between two magnetic impurities. But practically, doping two atoms is not impossible. Hence, calculating the RKKY interaction between n numbers of magnetic impurites are doped in a Weyl Semimetal is an area of research.

- We assumed the electrons are non interacting. But practically electrons do

interact. This may change the RKKY interaction.

- We assumed off resonant condition. Practically, this may not be always true.

Bibliography

[1] Binghai Yan and Claudia Felser. Topological materials: Weyl semimetals. *Annual Review of Condensed Matter Physics*, 8(1):337–354, 2017.

[2] A. A. Burkov. Chiral anomaly and diffusive magnetotransport in weyl metals. *Phys. Rev. Lett.*, 113:247203, Dec 2014.

[3] M. T. Béal-Monod. Ruderman-kittel-kasuya-yosida indirect interaction in two dimensions. *Phys. Rev. B*, 36:8835–8836, Dec 1987.

[4] LN Bulaevskii and SV Panyukov. Rkky interaction in metals with impurities. *JETP Lett*, 43(4):240–243, 1986.

[5] P. R. Wallace. The band theory of graphite. *Phys. Rev.*, 71:622–634, May 1947.

[6] Eugene Kogan. Rkky interaction in graphene. *Physical Review B—Condensed Matter and Materials Physics*, 84(11):115119, 2011.

[7] Mir Vahid Hosseini and Mehdi Askari. Ruderman-kittel-kasuya-yosida interaction in weyl semimetals. *Physical Review B*, 92(22):224435, 2015.

[8] Modi Ke, Mahmoud M Asmar, and Wang-Kong Tse. Nonequilibrium rkky interaction in irradiated graphene. *Physical Review Research*, 2(3):033228, 2020.

[9] Luca Chirolli, Fernando De Juan, and Francisco Guinea. Time-reversal and rotation symmetry breaking superconductivity in dirac materials. *Physical Review B*, 95(20):201110, 2017.

[10] Y Tamayama, T Nakanishi, K Sugiyama, and M Kitano. An invisible medium for circularly polarized electromagnetic waves. *Optics express*, 16(25):20869–20875, 2008.

[11] Elizabeth E Jenkins, Aneesh V Manohar, and Michael Trott. On gauge invariance and minimal coupling. *Journal of High Energy Physics*, 2013(9):1–28, 2013.

[12] Mark Semon and John Taylor. Thoughts on the magnetic vector potential. *American Journal of Physics*, 64:1361, 11 1996.

[13] Naoto Tsuji, Takashi Oka, and Hideo Aoki. Correlated electron systems periodically driven out of equilibrium: Floquet + DMFT formalism. *Phys. Rev. B*, 78:235124, Dec 2008.

[14] Hideo Aoki, Naoto Tsuji, Martin Eckstein, Marcus Kollar, Takashi Oka, and Philipp Werner. Nonequilibrium dynamical mean-field theory and its applications. *Rev. Mod. Phys.*, 86:779–837, Jun 2014.

[15] André Eckardt and Egidijus Anisimovas. High-frequency approximation for periodically driven quantum systems from a floquet-space perspective. *New Journal of Physics*, 17(9):093039, sep 2015.

[16] Marin Bukov, Luca D'Alessio, and Anatoli Polkovnikov and. Universal high-frequency behavior of periodically driven systems: from dynamical stabilization to floquet engineering. *Advances in Physics*, 64(2):139–226, 2015.

[17] Johannes Hausinger and Milena Grifoni. Dissipative two-level system under strong ac driving: A combination of floquet and van vleck perturbation theory. *Phys. Rev. A*, 81:022117, Feb 2010.